Shock-Tube Study of Vibrational Relaxation in Carbon Monoxide Using Pressure Measurements

RONALD K. HANSON*
NASA Ames Research Center, Moffett Field, Calif.

Measurements of pressure on the end wall of a shock tube have been used to infer the continuously varying rate of vibrational excitation behind incident shock waves in undiluted carbon monoxide. Results are presented in the form of separate relaxation-time plots for each shock wave studied. The data cover the temperature range 2400–6000°K and are in excellent agreement with the previous results of Matthews[1] and Hooker and Millikan.[2] The relaxation-time curves from all the experimental runs tend to fall on a single straight line on a conventional Landau-Teller plot, with the exception of data obtained near equilibrium. These results support use of the Landau-Teller rate equation to describe vibrational excitation in CO for situations involving large departures from equilibrium, but point out the possible need to modify the rate equation for situations in which the vibrational energy mode is highly excited.

Introduction

PAST investigations of vibrational relaxation in shock-heated gases have made extensive use of the Landau-Teller relaxation equation[3,4]

$$De_v/Dt = (\bar{e}_v - e_v)/\tau \qquad (1)$$

for the reduction of experimental rate data and for the calculation of flowfields. In this expression e_v is the vibrational energy of the gas and $\bar{e}_v$ its local equilibrium value. The parameter τ, generally called the relaxation time, is used to represent $\{k_{1,0}[1 - \exp(-\Theta_v/T)]\}^{-1}$ where $k_{1,0}$ is the usual transition probability per sec for a quantum transition between the first excited state and the ground state of a harmonic oscillator, T is the translational temperature, and Θ_v is the characteristic vibrational temperature of the oscillator. Equation (1) is strictly correct only for a system of harmonic oscillators undergoing weak interaction with an infinite heat bath of atoms,[4] but it is also frequently applied to the case of a pure gas where the heat bath is considered to be the translational and rotational energy modes of the molecules themselves. This may not be a suitable model for accurately describing the flow behind strong shock waves when the system is far from equilibrium or the temperatures are high enough to cause significant population of high-lying, anharmonic energy levels. Recent shock-tube experiments in O_2,[5] N_2[6] and CO[7,8] have presented evidence both for and against the adequacy of the Landau-Teller equation for such situations.

The object of the present study was to investigate the adequacy of the Landau-Teller equation for shock-heated CO, in particular for situations involving large departures from equilibrium. The approach used here was similar to that employed in the previously referenced works in that the rate of vibrational excitation was continuously determined as the temperature varied throughout the relaxation zone following an incident shock wave. However, the previous studies made use of optical measurement techniques, while the present investigation employed a record of the pressure history on a shock-tube end wall to infer the rate of vibrational excitation behind the incident shock wave.

Previous work on vibrational relaxation in shock-heated carbon monoxide has been reported by Matthews[1] and by Hooker and Millikan.[2] Matthews measured density changes behind incident shock waves, using a Mach-Zehnder interferometer, and inferred a single, average value of $P\tau$ vs temperature for each experiment. Hooker and Millikan observed the rate-of-rise of infrared emission behind incident shock waves in CO and related this to an average relaxation time for each set of shock conditions. In addition, by monitoring the emission from the fundamental and first overtone separately, Hooker and Millikan were able to demonstrate that the vibrational excitation most likely occurred by means of single-quantum transitions for the low-lying vibrational levels. Values for the relaxation times in the temperature range of overlap between these studies agreed to within 15%. On the basis of data from both studies, Hooker and Millikan[2] presented the best-fit expression

$$\log_{10}(P\tau,\text{atm-sec}) = 75.8T^{-1/3} - 10.16 \qquad (2)$$

which they estimated to be valid to within 10% over the temperature range for which data were presented, 1100°–4900°K. The results of the present study extend the temperature range for which CO data are available to 6000°K.

Theory

The experimental observable in this study was the time-varying pressure on a shock-tube end wall following reflection of the incident shock wave. The sensitivity of the end-wall pressure to relaxation processes behind incident shock waves has been demonstrated previously by Baganoff,[9,10] but application of the end-wall technique for accurate rate measurements has awaited a satisfactory theory for relating the rate-of-change of pressure to the appropriate relaxation rate in the gas. Numerical schemes have been developed for calculating the entire reflected-shock flowfield, including the end-wall pressure, in either a vibrationally relaxing gas[11] or a chemically relaxing gas,[12] but these techniques presently consume too much computer time to be useful for data-reduction purposes. The difficulty is that the reflection process is unsteady and cannot be viewed in the simple,

Received November 11, 1970; revision received June 1, 1971. Portions of this work were performed in the Department of Aeronautics and Astronautics at Stanford University, Stanford, Calif., under support from NASA Grant NGR 05-020-245. The author wishes to thank Prof. D. Baganoff of Stanford University and L. Presley of Ames Research Center for several valuable technical discussions and Mrs. E. Williams for her expert assistance with the computer programming.

Index Category: Shock Waves and Detonations; Thermochemistry and Chemical Kinetics.

* NRC Postdoctoral Fellow.

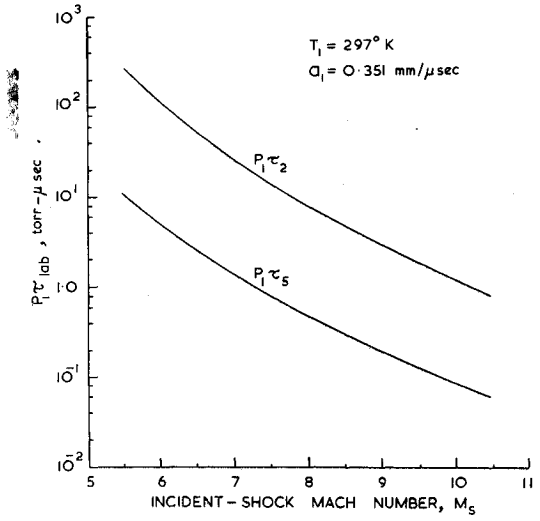

Fig. 1 Vibrational relaxation times in CO; the curves are for laboratory time, and are based on the rate expression in Eq. (2).

steady-coordinate manner usually employed with incident-shock relaxation studies.

Recently, it was observed that calculations of the end-wall pressure history could be greatly simplified in certain situations, and an appropriate theory suitable for such circumstances has been put forward.[13,14] The approximate theory has application for both vibrational and chemical relaxation in many common gases, and provides excellent agreement with the results of more lengthy numerical calculations.[11,12] A summary of the simple theory, as it pertains to a gas undergoing vibrational relaxation only, follows below.

The exact behavior of the end-wall pressure is rather complex, even with the assumption of inviscid-adiabatic flow imposed here, since relaxation processes continue simultaneously on both sides of the reflected shock wave as it moves away from the end wall. However, if the time scales of the relaxation processes behind the reflected shock, region 5, and ahead of the reflected shock, region 2, are different by at least an order of magnitude, then these effects can be considered separate, and the overall pressure history is greatly simplified. In such a case the wall pressure would have an initial value P_{F2-F5} corresponding to frozen vibrations in regions 2 and 5. The pressure would then decay,[9] in a time of order τ_5, to a level P_{F2-E5} corresponding to shock-wave reflection in a real gas where the vibrations are equilibrated (with the translational and rotational energy modes) in region 5 but remain frozen in region 2. The value of τ_5 is given approximately by substituting the frozen values of temperature and pressure (T_{F2-F5} and P_{F2-F5}) into an appropriate rate expression, e.g., Eq. (2) for the case of CO. On a longer time scale of order τ_2 the wall pressure would rise[9] to its final value, P_{E2-E5}, corresponding to the attainment of vibrational equilibrium both upstream and downstream of the reflected shock wave; and $P_{E2-E5} > P_{F2-F5}$. An estimate of τ_2 would be given by inserting the frozen values of temperature and pressure behind the incident-shock front (T_{F2} and P_{F2}) into the same rate expression and then converting from particle time to laboratory time.

Figure 1 presents calculated values for the laboratory relaxation times τ_2 and τ_5 in CO based on the rate expression of Eq. (2). These relaxation times were computed using the frozen shock conditions, and have been converted to laboratory time by assuming τ_5 is equal to $\tau_{5\text{particle}}$ and τ_2 is equal to $\tau_{2\text{particle}}/\eta_F$, where η_F is the frozen value for the density ratio across the incident shock wave. Note that both τ_2 and τ_5 are scaled by the initial shock-tube pressure. The ratio τ_2/τ_5 varies from about 13 at $M_s = 10$ to about 27 at $M_s = 5.5$, so the assumption of separate relaxation time scales should be reasonably valid within this range.

For situations in which the relaxation times τ_2 and τ_5 differ by more than an order of magnitude, it is possible to select test conditions wherein the relaxation time in region 2 may be adequately resolved while the relaxation time in region 5 is smaller than the temporal resolution of the end-wall instrumentation. Under these conditions, the relaxation zone following the reflected shock wave is negligibly thick; i.e., the gas throughout region 5 would appear to remain in local vibrational equilibrium. On the time scale of interest, τ_2, the measured wall pressure would begin at about P_{F2-E5} and thereafter rise asymptotically to P_{E2-E5}. In the paragraphs that follow, we shall construct a mathematical model which is exact at large time, i.e., near equilibrium, for predicting the reflection process under the above conditions, and the solutions are appropriately termed "outer" solutions.

The model for the reflection process is most conveniently discussed using the x-t diagram of Fig. 2 where x refers to the distance from the shock-tube end wall and t to the time after reflection of the incident shock wave. The incident shock wave is assumed to travel toward the end wall at a constant speed V_s and to reflect with a constant speed V_r, taken here to be the final equilibrium value of shock speed corresponding to vibrational equilibrium upstream and downstream of the reflected shock wave, i.e., $(V_r)_{E2-E5}$, as will be discussed later. Also shown in the diagram is a typical density (ρ) profile in region 2, which would appear as if it were travelling across the x-t plane "attached" to the incident shock wave. The significance of points A,B,C and D follows from the technique employed to map the spatial variations in flow properties throughout region 2 into temporal variations in pressure on the end wall after shock-wave reflection.

The first step in the mapping process consists of projecting the properties at point A across the x-t plane to form the upstream conditions for the reflected shock wave at point B. The state of the gas at point C immediately behind the reflected-shock front is then known from real-gas shock-jump relations since the gas is assumed to be in local vibrational equilibrium. The pressure at point C can be transferred across region 5 along a characteristic terminating at point D. The pressure is unchanged along this characteristic save for small variations accounting for any change in particle velocity. The characteristics may be considered straight for all practical purposes, with a slope equal to the equilibrium speed of sound, since only small variations in temperature and particle velocity occur in region 5 for this problem. The complete wall-pressure history can be constructed from a number of these transformations, each originating at a different position behind the incident shock wave. A given pressure history therefore corresponds uniquely to a particular variation in the rate of vibrational excitation across region

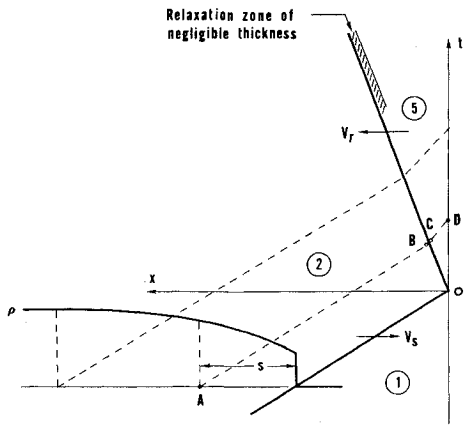

Fig. 2 (x − t)-diagram of shock-wave reflection.

2. In fact, with the assumptions, or approximations, made here the rate-of-change of pressure at point D can be written explicitly in terms of the gradient in density or vibrational energy at point A, as shown below.[14]

The pressure at point C is given by standard shock-jump relations[15] as

$$P_C = P_B + \rho_B(U_B + V_r)^2(1 - \rho_B/\rho_C) \tag{3}$$

where, from the conservation of mass,

$$\rho_B/\rho_C = (V_r + U_C)/(V_r + U_B) \tag{4}$$

In these relations U_B is the speed of the gas toward the end wall at point B

$$U_B = V_s(1 - \rho_1/\rho_B) \tag{5}$$

and U_C is the speed of the gas toward the wall at point C. Numerous calculations for typical equilibrium conditions at point C have shown that $U_C \ll V_r$, so the ratio ρ_B/ρ_C is well approximated by

$$\rho_B/\rho_C = V_r/(V_r + U_B) \tag{6}$$

The last result is physically reasonable since the flow in region 5 should be nearly stagnant with the exception of the narrow relaxation zone whose thickness we have neglected.

From incident-shock relations, one can write[15]

$$P_B = P_1 + \rho_1 V_s^2(1 - 1/\eta_B) \tag{7}$$

where the symbol η_B is used to denote the local value for the density ratio across the incident shock wave, ρ_B/ρ_1. Upon substitution of Eqs. (5–7), Eq. (3) becomes simply

$$P_C = P_1 + \rho_1 V_s^2(\eta_B - 1)(1 + V_r/V_s) \tag{8}$$

where $(1 + V_r/V_s)$ is a constant because of the assumption imposed on the reflected shock speed. Furthermore, $P_C/P_1 \gg 1$ for the shock strengths of interest here, so that one has the simple result

$$P_C/P_{E2\text{-}E5} = P_C/P_\infty = (\eta_B - 1)/(\eta_{E2} - 1) \tag{9}$$

The subscript ∞ has been used to denote the equilibrium state in region 5 previously labelled $E2$-$E5$. The correct asymptotic behavior of this last expression is obvious.

Since the velocity U_C was taken as zero, P_D may be set equal to P_C, and the slope of all right-running characteristics in region 5 may be approximated by a_∞, the equilibrium speed of sound calculated at the final equilibrium temperature in region 5. (For a discussion of the equilibrium speed of sound in a vibrationally relaxing gas, see Vincenti and Kruger.[15]) These last steps permit simple relations between P_D and η_A and between t_D and s_A. The rate-of-change of pressure on the end wall at point D can now be written directly in terms of the gradient in density at point A in region 2, i.e.,[14]

$$\frac{\partial}{\partial t}\left(\frac{P}{P_\infty}\right)_D = \frac{1 + V_r/V_s}{1 + V_r/a_\infty}\left[V_s \frac{\partial}{\partial s}\left(\frac{\eta - 1}{\eta_{E2} - 1}\right)\right]_A \tag{10}$$

In terms of the substantial derivative, this last equation becomes

$$\frac{\partial}{\partial t}\left(\frac{P}{P_\infty}\right)_D = \frac{\eta_A}{\eta_{E2} - 1}\left(\frac{1 + V_r/V_s}{1 + V_r/a_\infty}\right)\left(\frac{D\eta}{Dt}\right)_A \tag{11}$$

To obtain an expression relating the rate-of-change of pressure on the end wall to the rate-of-change of vibrational energy behind the incident shock wave, we now need an expression relating $(D\eta/Dt)$ to (De_v/Dt). Manipulation of the usual conservation relations,[15] the thermal equation of state

$$P = \rho RT \tag{12}$$

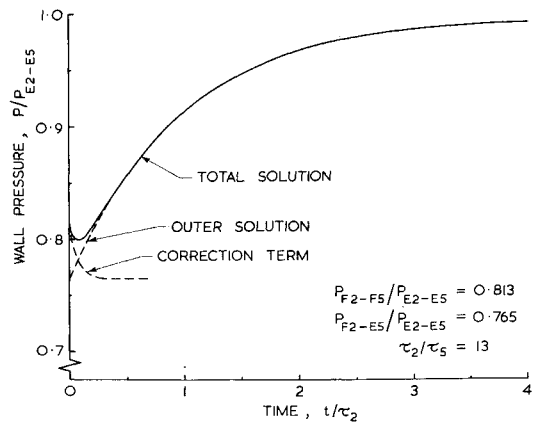

Fig. 3 Estimate of the error involved in an outer solution for $M_s = 10$ in CO.

and the caloric equation of state

$$h = (\tfrac{7}{2})RT + e_v \tag{13}$$

yields the relation

$$\frac{e_v}{\gamma RT_1/(\gamma - 1)} = 1 + (\gamma - 1)M_s^2\left(\frac{1 - 1/\eta^2}{2}\right) - \frac{1 + \gamma M_s^2(1 - 1/\eta)}{\eta} \tag{14}$$

where T_1 is the temperature of the gas at the initial shock-tube conditions, γ is the specific-heat ratio in the unexcited gas ($\frac{7}{5}$ for CO), and M_s is the Mach number of the incident shock wave based on $M_s = V_s/(\gamma RT_1)^{1/2}$. Thus, the specification of η at any point A in the incident flow (from a measurement of P_D) uniquely determines all other thermodynamic quantities at that point, including the vibrational energy per unit mass, e_v. The desired relation for $(D\eta/Dt)$ is easily shown to be

$$\frac{D\eta}{Dt} = \frac{De_v}{Dt}\Big/\frac{de_v}{d\eta} = \frac{(\gamma - 1)\eta^2}{\gamma RT_1}\left[1 + M_s^2\left(\gamma - \frac{\gamma + 1}{\eta}\right)\right]^{-1} \times \frac{De_v}{Dt} \tag{15}$$

Substitution of Eqs. (1) and (15) into Eq. (11) provides a direct relation between the observed rate-of-change of pressure (at D) and the characteristic relaxation time for a known set of thermodynamic conditions (at A). In practice these calculations can be carried out with a computer program based on the above equations and the experimental observations; the result is a continuous plot of $P\tau$ vs T(or $T^{-1/3}$) for the entire relaxation zone behind the incident shock wave.

A few comments should be made with regard to the error in wall pressure associated with the three important approximations of: 1) neglecting the relaxation time in region 5; 2) assuming constant reflected-shock velocity; and 3) assuming that $U_C = 0$. A crude estimate of the error which results from setting the relaxation time in region 5 equal to zero is presented in Fig. 3 for the case of a Mach 10 shock wave. This case provides a conservative test of the theory since the ratio τ_2/τ_5 takes on its smallest value for the range of experiments reported here. For purposes of this error estimate only, the "actual" pressure solution is calculated by simply adding an approximate correction term to the outer solution. We assume that to first order the correction term, intended to account for the effects of relaxation in region 5, is independent of the outer solution. The outer solution may be approximated by

$$P_0 = P_{F2\text{-}E5} + (P_{E2\text{-}E5} - P_{F2\text{-}E5})(1 - e^{-t/\tau_2}) \tag{16}$$

and a reasonable form for the correction term is

$$P_c = (P_{F2\text{-}F5} - P_{F2\text{-}E5})e^{-t/\tau_5} \quad (17)$$

τ_2 and τ_5 are the previously defined laboratory relaxation times.

The total or "actual" solution for the wall pressure is therefore

$$P_t = P_0 + P_c \quad (18)$$

and the normalized error introduced by employing the outer solution only is simply $P_c/(P_0 + P_c)$. This error is clearly negligible for values of t/τ_2 greater than about $\frac{1}{4}$, as shown in Fig. 3. More important for the present application, however, is the difference in slope owing to the correction term, i.e.

$$\left|\frac{\partial P_c/\partial t}{\partial P_t/\partial t}\right| \simeq \left|\frac{\partial P_c/\partial t}{\partial P_0/\partial t}\right| = \frac{(P_{F2\text{-}F5} - P_{F2\text{-}E5})e^{-t/\tau_5}/\tau_5}{(P_{E2\text{-}E5} - P_{F2\text{-}E5})e^{-t/\tau_2}/\tau_2} \quad (19)$$

Substitution of values appropriate for this case yields

$$\left|(\partial P_c/\partial t)/(\partial P_0/\partial t)\right| = 2.6\exp(-12t/\tau_2) \quad (20)$$

which decays to 2% by $t \simeq 0.4\tau_2$. The outer-solution model thus yields accurate results, even for this conservative case, at times much smaller than τ_2. For the single experiment conducted at Mach 10 in this investigation $P_1 = 2$ torr and $\tau_2 \simeq 0.6$ μsec, so the "error" in slope decreases to 2% within 0.24 μsec, which is only slightly larger than the response time of the instrumentation employed. The above solution is not an exact representation of the actual pressure history, but does provide a measure of confidence in the use of the outer-solution technique.

The second major assumption of a constant-speed reflected shock wave is an approximation which improves as time increases and need be questioned only for short times. Actually, the reflected shock wave moves away from the end wall with an initial velocity $(V_r)_{F2\text{-}F5}$ which rapidly decays, in a time of order τ_5, toward a value of $(V_r)_{F2\text{-}E5}$. Then on a time scale of the order of τ_2, the shock speed increases to a final value $(V_r)_{E2\text{-}E5}$; however, there is little difference between $(V_r)_{F2\text{-}E5}$ and $(V_r)_{E2\text{-}E5}$ for the conditions of this study. The maximum error in pressure (consistent with the neglect of τ_5) can be estimated by using the $(V_r)_{F2\text{-}E5}$ value of shock speed in Eq. (3) rather than the assumed value of $(V_r)_{E2\text{-}E5}$. The resulting differences in the magnitude and slope of the wall pressure are less than 1% over the range of shock speeds employed in the present study.

The last major approximation was the neglect of a finite value for U_C, and the resulting error in the pressure at point D is approximately

$$\Delta P/P_D \simeq \rho_C U_C a_\infty/P_D \simeq \gamma U_C/a_\infty \quad (21)$$

Several calculations for equilibrium conditions at point C have indicated that this ratio is less than 1% in magnitude. Fortunately, the errors involved in these last two major approximations effectively cancel since they are of opposite sign and of nearly equal magnitude.

Finally, it should be noted that the theoretical model has not accounted for heat-transfer effects and the well-known interaction between the reflected shock wave and the side-wall boundary layer. This latter effect can be dismissed in the present study because of the time scale involved. The observations are typically less than 8 μsec in duration, and this is less time than that required for a disturbance to propagate from the side wall (through either the gas or the gauge) to the axis of the tube where the pressure sensor is located.

Heat transfer to the end wall causes a decrement in wall pressure proportional to $t^{-1/2}$. An estimate of the time required for the perturbation to decay to 5% can be made from Baganoff's calculations for nitrogen (see Fig. 7 of Ref. 9), namely about 0.4 μsec/torr of initial pressure for the shock speeds of interest in this work. This is a conservative figure, however, as Baganoff's calculations were based on frozen conditions in region 5. Calculations using the thermodynamic state appropriate here ($F2$-$E5$) should yield a more favorable, smaller value. Since all the present experiments, except 3 at high Mach numbers, were conducted at pressures between 4 and 20 torr, this effect can reasonably be neglected. An accurate quantitative prediction of the effects of end-wall heat transfer upon the wall pressure, especially at short times after reflection, must await the development of an adequate physical model for heat transfer in a nonequilibrium gas.

Experimental Technique

The shock tube used for these measurements is located in the Aerophysics Laboratory at Stanford University. The driven section is a tube of extruded aluminum with inside dimensions of 2.0 × 2.0 in. and a length of 25 ft. Sufficiently strong shock waves were generated by operating the tube in the combustion-driven mode using a stoichiometric mixture of hydrogen and oxygen diluted with helium. The mixtures were ignited by pulsing simultaneously 8 spark plugs arranged around the 3-in.-diam stainless-steel driver chamber.

Incident-shock speeds were varied from 2.3 to 3.5 mm/μsec, corresponding to Mach numbers between 6.5 and 10, and were measured using 4 piezoelectric pressure sensors spaced along the last 16 in. of the driven tube upstream of the end wall. The uncertainty in the measured shock speed was less than 1%. Shock-speed attenuation, a common handicap of combustion-drive operation, varied up to 2% per ft, depending on the test conditions. For the brief test times of interest here, however, this effect can be neglected in the data analysis.

Initial pressures in the driven section ranged from 2 to 20 torr and were measured with either a McLeod gauge or a Wallace and Tiernan pressure gauge which was calibrated against the McLeod gauge. The maximum error in the recorded pressure is estimated, primarily on the basis of a cross-calibration of 3 separate McLeod gauges, to be about 1%.

The test gas was drawn from a cylinder of Matheson Research Grade Carbon Monoxide with the following analysis provided by the manufacturer: $CO_2 < 10$ ppm, $O_2 < 15$ ppm, $N_2 < 300$ ppm, Ar < 10 ppm, $H_2 < 5$ ppm, and a dew point below −80°F. The CO was admitted to the shock tube after passage through a 10-ft coil of copper tubing immersed in liquid nitrogen. The results of a few tests made without this cold trap are also discussed below.

Since the shock tube was combustion driven, great care was taken to remove the water vapor present after each run. Immediately after each firing the tube was cleaned thoroughly with cheesecloth and pumped down, first with a mechanical pump and then with a diffusion pump, to a final pressure of about 10^{-5} torr. Pumping always continued for at least one hour between runs and in many cases continued overnight. The apparent leak rate after one hour of pumping, owing to outgassing and vacuum leaks, was measured to be less than 2×10^{-4} torr per min. Since the total elapsed time between isolating the vacuum system and firing the tube was about 5 min, the total level of contamination from this source should have been less than 10^{-3} torr.

The pressure gauge employed was a modified version[16] of the gauge developed earlier by Baganoff.[10] In brief the gauge consists of a thin, capacitive-type strain-sensing element bonded to the front face of a 3-in.-diam cylinder of Lexan plastic which forms the end wall of the shock tube. The sensing element is a parallel-plate capacitor composed of a film of Lexan plastic (0.003-in.-thick) with a layer of copper foil (0.0001-in.-thick) bonded to each side. One layer of foil serves as the ground element and is a full 3-in. in diameter. The other layer of foil consists of two half-circles, slightly separated, that form a near circle of 0.62-in.-diam.

One or both of these elements may be charged to high voltage, the dual elements providing a simple scheme for removing any noise present owing to charged particles in the gas.[16] The capacitor is charged with a precision power supply so that the final capacitor voltage (up to ± 3 kV) is accurately known.

Changes in the gas pressure adjacent to the end wall cause small variations in the thickness of the dielectric slab between the foil electrodes, thus creating (temporarily) a proportionate change in the voltage on the charged electrode. Changes in the voltage are transmitted to a cathode follower and then to an oscilloscope for recording. The primary limitation of this gauge is the short observation time obtainable. This limitation is imposed by the arrival at the small sensing element of a tension wave, originating at the intersection of the gauge face and the shock-tube side wall, which destroys the one-dimensional character of the compression within the capacitor. For a 2 in. shock tube the observation time is limited to about 10 μsec, while for a 6 in. tube (and gauge diameter) the limit would be about 30 μsec.

The gauge performance is illustrated in Fig. 4 which presents the response to an applied step in pressure. The step was obtained using a weak shock wave and a high initial pressure so that real-gas effects could be neglected. The rise time is seen to be about 0.1 μsec. Such pressure steps provide a convenient means of calibrating the gauges since the magnitude of the step is known from standard relationships once the initial pressure and shock speed have been measured. The gauge response has been shown[10,16] to be quite linear with respect to pressure and capacitor voltage. A typical calibration constant is about 0.6 mV/psi/kV of charging voltage.

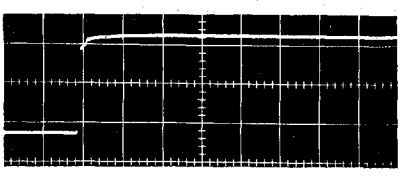

Fig. 4 Response of the pressure gauge to a pressure step; sweep speed is 1 μsec/div.

Results

Typical data are displayed in Fig. 5. Aside from a small amount of "ringing" in the signal immediately following reflection, the character of these traces is in good accord with that predicted by the simple theory discussed previously. A small amount of overshoot was present in some cases, i.e., Figs. 5(a) and 5(c) which were obtained with the same pressure gauge. The ringing pattern for a given gauge was quite repeatable, however, so that this effect upon the data could be minimized by considering the response of that same gauge to a known pressure signal, for example the pressure step used for calibration.

Vibrational equilibrium corresponds to the point where the oscilloscope trace reaches a steady, asymptotic value. The experiments were usually designed so that equilibrium was effectively reached within the useful observation time of the gauge. A comparison of the theoretical and measured equilibrium pressures could then be used to provide a simple check on the quality of a particular run.

The data-reduction process required four steps. First, the pressure trace was accurately read from the oscillogram using an optical comparator with an $(x$-$y)$-coordinate printout, and the pressure values were normalized by dividing each reading with the final, asymptotic pressure reading. Secondly, an instrument correction factor was applied to those readings within the first microsecond or so after reflection. This factor was taken, as a first approximation, to be the ratio of the ideal response and the response actually

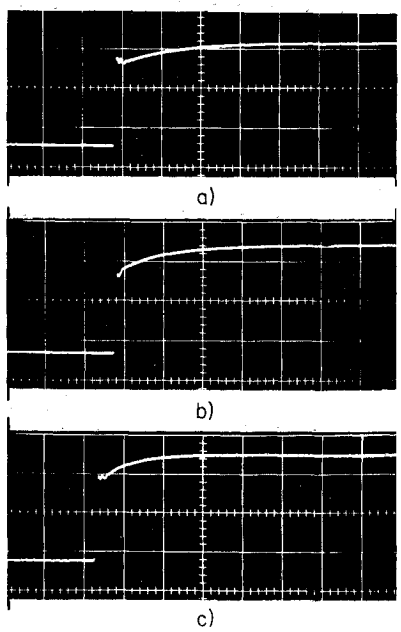

Fig. 5 Wall-pressure histories in vibrationally relaxing CO: a) $M_s = 7.4$, $P_1 = 10$ torr; b) $M_s = 8.4$, $P_1 = 5$ torr; and c) $M_s = 10.0$, $P_1 = 2$ torr; sweep speeds are 1 μsec/div.

recorded (at a given instant after shock reflection) when a step in pressure was applied to that gauge. Any distortion in the relaxation-time data, caused by the short-time behavior of the gauge, was thereby minimized. The third step in the data reduction consisted of fitting (with least-mean-square deviation) an eighth-order polynomial through the data using a computer technique. The result was an analytical expression for P/P_∞ vs time which accurately represented the data and could be differentiated to determine the rate-of-change of pressure at any instant. Finally, the fourth step consisted of submitting this polynomial into a computer program based on the theoretical model discussed earlier, along with the initial conditions of temperature, pressure and shock speed, to yield a continuous plot of relaxation time versus translational temperature throughout the relaxation zone.

The ability of the data-reduction technique to reproduce an assumed variation of $P\tau$ was checked by computing a hypothetical end-wall pressure signal using the outer solution and Eq. (2). These "data" were then subjected to the same steps leading to a polynomial curve fit. Submission of this polynomial to the final computer program yielded values for $P\tau$ agreeing to better than 1% with Eq. (2) for temperatures corresponding to values of $P/P_\infty < 0.99$. Since the final results for $P\tau$ based on the present measurements were all obtained for values of $P/P_\infty \lesssim 0.98$, the error introduced by the polynomial curve fit was negligible. (Actual pressure data are simply not reliable enough to be used for calculating the rate-of-change of pressure when P/P_∞ is greater than about 0.98, owing primarily to the inaccuracies associated with reading data from an oscilloscope trace and the possible influence of nonideal shock-tube effects on the test gas located farthest from the incident-shock front.) It should also be noted that several attempts were made to fit the data with exponential-type expressions, since such curve fits were successfully applied in previous studies[7,8] involving density measurements, but these attempts invariably yielded poorer data fits than those obtained with high-order polynomials. Exponential curves were satisfactory for fitting segments of the data traces but not for fitting an entire pressure history.

The selection of the optimum polynomial to fit the dimensionless pressure data was made by varying the order of the polynomial

$$P/P_\infty = b_0 + b_1 t + b_2 t^2 + \ldots + b_n t^n \qquad (22)$$

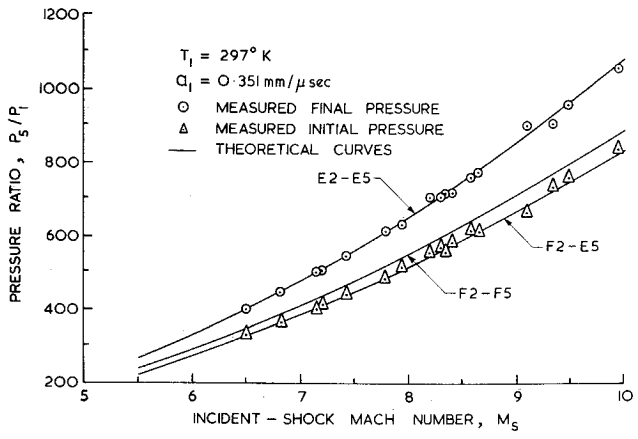

Fig. 6 Initial and final pressure levels in vibrationally relaxing CO.

where n is the order and t is the time after reflection, and inspecting the statistical quality of the resulting data fits for several sets of pressure data. A value of n equal to 8 was finally selected as providing the optimum data fit from the viewpoints of accuracy and computer time. The root-mean-square deviation of pressure data fit with an eighth-order polynomial (based on about 40 data points per pressure history) was typically less than 10^{-3} of the equilibrium pressure, and the computer time required to fit a single set of data was somewhat less than a minute. The deviation generally increased about 50% as the polynomial order was dropped to 5. However, polynomials of order 5 to 7 yielded nearly the same values of slope (within a few percent) as a polynomial of order 8, except for small values of t where the rate-of-change of pressure was greatest. Higher orders than 8 generally provided negligible improvement in the quality of the data fit. The curve fits accepted for the next stage of data reduction were in all cases well within the slight scatter of the data points.

Before a run was submitted to the data-reduction scheme, a comparison was made between the measured value for the equilibrium pressure and the theoretical value based on the measured shock speed and initial pressure. The maximum deviation was about 3%, as shown in Fig. 6, a difference which is compatible with the quoted tolerances on the measurements of shock speed and initial pressure. Also shown in Fig. 6 are approximate experimental points for the pressure level immediately after reflection. These were inferred, after applying the instrument correction factor, by extrapolating the data points back to time zero. While these results for the initial pressure are less accurate than those for the final pressure, because of the extrapolation necessary, there appears to be good agreement over the full range of experiments with the theoretically predicted value, $P_{F2\text{-}E5}/P_1$. Certainly, the agreement between experiment and theory shown in Fig. 6, for both the initial and final pressure levels, provides substantial confidence in the theoretical model and the experimental technique.

Final results of the CO experiments are presented in the form of a conventional Landau-Teller plot in Fig. 7. Individual curves from a few of the experiments have been omitted because they overlapped other curves, thus adding no new information while making the plot difficult to follow. Also shown are the individual points found by Matthews[1] and the straight-line fit suggested by Hooker and Millikan.[2] The majority of the individual curves are in good agreement with this fit, especially at higher temperatures, although there is a general tendency near equilibrium for a "hook" to appear which corresponds to a decrease in the local value of the relaxation time as defined by Eq. (1). If the physical model which leads to both the Landau-Teller rate equation and the temperature dependence of Eq. (2) is correct, of course, all the experimental results should collapse onto a single straight line in Fig. 7, for example the curve suggested by Hooker and Millikan. The fact that the present data follow Hooker and Millikan's curve rather closely thus substantiates, within experimental error, the essential accuracy of the Landau-Teller equation for describing shock-wave relaxation zones in CO. The agreement found at the high-temperature end of each individual experiment curve is particularly important since this confirms the adequacy of the rate equation for situations involving large departures from equilibrium. The presence of the small hook near equilibrium, however, provides some evidence that the Landau-Teller equation may need to be modified when the vibrational energy mode is highly excited.

Great care has been taken to check that these hooks were not an artifact of the data-reduction scheme, or a result of some nonideal shock-tube phenomenon, since this behavior of the relaxation time is precisely the type of information needed to suggest modifications to Eq. (1). The difficulty of confirming and quantifying this behavior, however, is that the relaxation-time results are less reliable near equilibrium where a small error in the pressure measurement or the curve fit can produce a large error in $P\tau$. For example, a small systematic error in selecting the correct asymptotic value for P_∞ could lead to a consistent overestimate of the rate-of-change of pressure near equilibrium, although a careful investigation has indicated that reasonable variations in the asymptote selected are insufficient to cause a large effect in data restricted to values $P/P_\infty < 0.98$. Furthermore, no consistent pattern of deviation between the measured and theoretical asymptotes was indicated in Fig. 6. The effect of changing the order of the polynomial was also checked and found to produce only small changes in the plotted results of Fig. 7. In all cases the polynomial fits were plotted for direct comparison with the experimental data in order to minimize the possibility of systematic errors and to be certain that the curve fit was a valid representation of the actual data. The polynomials invariably yielded monotonic changes in P/P_∞ and $d(P/P_\infty)/dt$ throughout the useful portion of the pressure histories (i.e., there were no oscillations in pressure or the rate-of-change of pressure between points). It is also worth noting that the hooks first appeared (in the experiments of Fig. 7) at values of P/P_∞ of about 0.92–0.95 ($T_{E2}/T \simeq$ 0.93–0.96), where the level of confidence in the plotted results was quite high, and that a continuation of the curves for values of P/P_∞ greater than 0.98 always resulted in an extension of the hooks. The evidence is thus rather convincing,

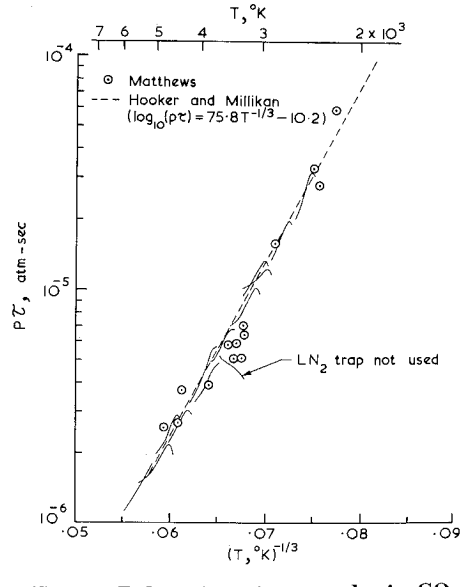

Fig. 7 Relaxation-time results in CO.

in the author's opinion, that the effect is real. In addition, similar observations of hooks have been reported by Appleton[6] and Hanson and Baganoff[17] in investigations of vibrational relaxation in N_2, so the present results are not entirely without precedent.

Appleton found hooks present over the full range of his experiments (3000°–9000°K), but the effect he observed was significantly more pronounced for temperatures above 5500°K. Such results led him to the tentative conclusion that the relaxation time was dependent on the degree of vibrational excitation as well as the translational temperature. His work, and the present study, might thus be taken to imply that the transition probabilities for vibrational excitation should increase more rapidly than linearly with the vibrational quantum number, as is assumed in the usual derivations of Eq. (1). The result of increasing the upper-level transition probabilities in the harmonic-oscillator model, or of allowing for multiple quantum jumps and anharmonicity, could lead to an appropriate new rate equation with a relaxation time depending on both the translational temperature and the degree of vibrational excitation, although most certainly the elegant simplicity of the Landau-Teller equation would be lost. Additional experiments are clearly needed before quantitative corrections to the Landau-Teller rate equation can be established.

The influence of impurities must also be examined as a possible explanation for the decrease in relaxation time, and the results found here with respect to impurities emphasize their importance rather clearly. As noted previously, the shock tube was carefully cleaned after each run and the gas was admitted to the tube through a liquid-nitrogen cold trap. Two runs were made without the cold trap, however, and Fig. 8 presents the results for one of these runs. A visual inspection detected no significant variations between this record and previous records obtained with the cold trap at the same shock conditions. Only later when these runs were analysed by the complete data-reduction scheme was any difference noted. The rather striking results of one such run are shown in Fig. 7 with the label "LN_2 trap not used." Although the relaxation-time curve begins with a reasonable value at the high-temperature end, the relaxation time decreases steadily throughout the relaxation zone. It is also noteworthy that both of the runs with nontrapped CO were made at the same shock conditions and yielded nearly identical results on the Landau-Teller diagram.

In retrospect, the results obtained without a cold trap seem quite reasonable for situations wherein an impurity such as water vapor is present. Unfortunately the actual extent and identity of the impurities present in these cases are not known. The question of the possible influence of impurities for cases in which a trap was employed also cannot be answered definitely. It is possible that some impurity (or its dissociation products) was present even after trapping, and that this source provided a small quantity of very efficient collision partners. If some threshold concentration is necessary for this collision partner to be rate controlling, then both the hook that forms late in the relaxation as well as the negative slope of the nontrapped runs could be due to the same impurity effect. However, due to the small probable impurity level in the trapped runs, and the resultant large increase that would be required for the collision efficiency of the impurity or its reaction products, it is not

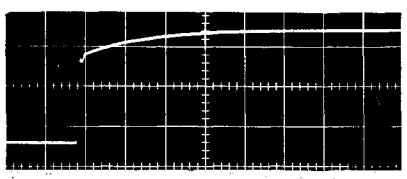

Fig. 8 Wall-pressure history in impure CO; M_s = 7.8, P_1 = 5 torr CO, sweep speed = 1 μsec/div.

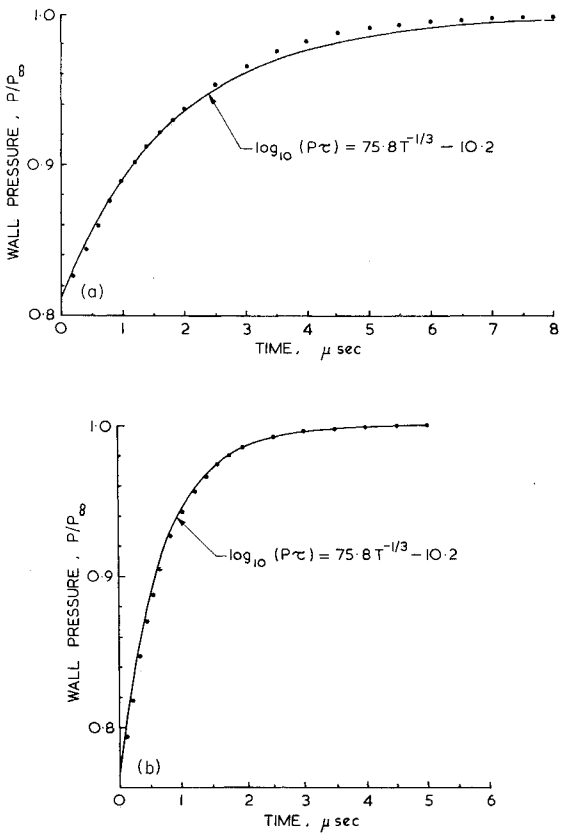

Fig. 9 Comparison of measured and calculated pressure histories in pure CO: a) M_s = 7.4, P_1 = 10 torr; and b) M_s = 10.0, P_1 = 2 torr.

believed at present that the hooks are due to impurities. Clearly, as already noted by many investigators, one must exercise great caution with respect to impurities in shock-tube experiments.

In spite of the hooks visible in Fig. 7, the overall agreement with a single curve drawn through all the data is quite good, most differences being less than the experimental error, and we thus conclude that the Landau-Teller rate equation provides an accurate description of bulk-macroscopic properties behind strong shock waves. The overall suitability of the rate equation in its present form is best demonstrated by comparing some measured pressure histories with those calculated (using the outer-solution technique) on the basis of Eq. (1) and the rate-expression in Eq. (2).

Figure 9(a) provides a comparison for the trace shown in Fig. 5(a) (see also Fig. 7, the fifth curve from the top). The experimental results are shown in the form of representative points taken from the corrected data. Many more points were of course used to find the curve fit through the data. The differences between the measured and calculated results are quite small and could, in any single case, be entirely due to experimental error. However, the pattern seems repeatable enough over several runs to suggest that the differences near equilibrium are real, and hence that some type of hook should appear on the curves in Fig. 7. Figure 9(b) presents a comparison for the trace shown in Fig. 5(c) (the strongest shock wave plotted in Fig. 7, i.e., the curve nearest the bottom). There is essentially no difference in slope throughout this pressure history, which is consistent with the agreement shown in Fig. 7. Since this is the only experiment which did not yield a hook in Fig. 7, and it is also the experiment with the strongest shock wave and the lowest initial pressure, it is felt that nonideal shock-tube effects may be responsible for the apparent disappearance of the hook. Figure 10 provides a similar comparison for one of the runs made without a cold trap (see Fig. 8). The effect of only a small amount

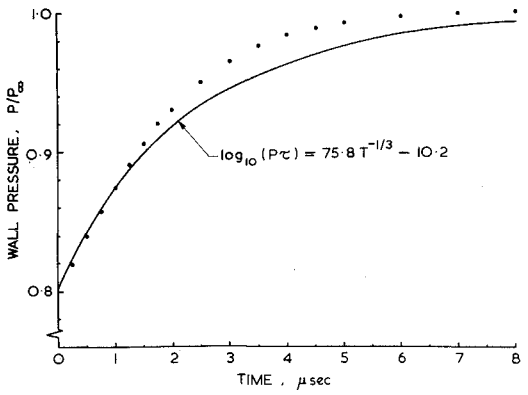

Fig. 10 Comparison of measured and calculated pressure histories in impure CO; $M_s = 7.8$, $P_1 = 5$ torr.

of impurities is, by comparison with the agreement shown in Fig. 9, quite pronounced.

The results shown in Fig. 9 demonstrate quite clearly the experimental accuracy required to detect any deviation from Landau-Teller behavior. Certainly, the technique employed here has been pushed to the limit of its present capability, and the advantages of this technique over some others are noteworthy. The time resolution is excellent, for example, and the location of the gauge sensor on the axis of the shock tube permits sampling of gas which has been processed entirely within the core of the flow; thus problems of shock-wave curvature and side-wall boundary layers are minimized. The primary disadvantage of this technique, of course, is that only macroscopic variations in the flowfield are detected. In order to provide detailed information of the vibrational relaxation of the gas, and hence to test the validity of the Landau-Teller rate equation on a microscopic basis, an experimental technique that would provide time-resolved information on the number densities in several vibrational energy states would be needed. However, as shown in this paper, careful use of an instrument that is sensitive to a macroscopic variable, such as the density or the total vibrational energy, can provide some insight into the microscopic behavior of the gas.

Conclusions

Measured pressure histories on the end wall of a shock tube have been used to infer the rate of vibrational excitation behind incident shock waves in undiluted carbon monoxide. Results for the characteristic relaxation time in the temperature range 2400–6000°K have been presented and shown to be in good agreement with the data of previous investigations employing different experimental techniques. The Landau-Teller rate equation has been verified for describing the vibrational excitation process in CO throughout most of the incident-shock relaxation zone, including conditions far from equilibrium. The results also substantiate over the temperature range investigated the linear dependence of $\ln(P\tau)$ on $T^{-1/3}$ predicted by the classical Landau-Teller theory. Thus, the end-wall measurement technique has been shown to be an accurate means of obtaining relaxation-rate information for cases in which a theoretical model of shock-wave reflection is available.

Evidence has also been presented to show that the relaxation times inferred with the Landau-Teller equation decrease near equilibrium, and hence that a properly defined relaxation time should depend on the degree of vibrational excitation as well as the local translational temperature. These results are similar to those reported by Appleton[6] in a study of vibrational relaxation in N_2 and lead one to consider modifying the rate equation to account for anharmonicity and increased values for the excited-state transition probabilities.

A pronounced decrease in relaxation time was noted when the CO was not passed through a liquid-nitrogen cold trap, the decrease being attributed to the importance of condensable impurities. The possible effect of impurities upon relaxation histories obtained with a cold trap has not been quantitatively defined. However, due to the low contamination levels in the test gas, the effects of the impurities are not believed the source of the hooks. Clearly, a careful study of vibrational relaxation wherein the impurity effects are quantitatively evaluated is in order.

Finally, it is interesting to speculate that the effect which leads to a decrease in relaxation time near equilibrium for an excitation flow process is related to the apparent discrepancy between relaxation times measured in shock-heated flows and expanding flows. This connection seems plausible since the effect found in the present work appears to depend upon the population density in excited vibrational states, and this population density is always larger than its local equilibrium value in an expanding flow. Hence, the relative influence of the excited-state population might be greater in a flow undergoing vibrational de-excitation rather than excitation. Additional experiments are definitely needed to assist in resolving these questions, and in particular it would be useful to obtain vibrational relaxation data, over a wide range of temperatures, for a gas only slightly perturbed from an initial, high-temperature equilibrium state. Experiments designed to yield such near-equilibrium rate data are currently being planned.

References

[1] Matthews, D. L., "Vibrational Relaxation of Carbon Monoxide in the Shock Tube," *Journal of Chemical Physics*, Vol. 34, No. 2, 1961, pp. 639–642.

[2] Hooker, W. J. and Millikan, R. C., "Shock-Tube Study of Vibrational Relaxation in Carbon Monoxide for the Fundamental and First Overtone," *Journal of Chemical Physics*, Vol. 38, No. 1, 1963, pp. 214–220.

[3] Landau, L. and Teller, E., "Contribution to the Theory of Sound Dispersion," *Physikalische Zeitschrift der Sowjetunion*, Vol. 10, 1936, p. 34.

[4] Clarke, J. F. and McChesney, M., *The Dynamics of Real Gases*, Butterworths, London, 1964.

[5] Lutz, R. W. and Kiefer, J. H., "Structure of the Vibrational Relaxation Zone of Shock Waves in Oxygen," *The Physics of Fluids*, Vol. 9, No. 9, 1966, pp. 1638–1642.

[6] Appleton, J. P., "Shock-Tube Study of the Vibrational Relaxation of Nitrogen Using Vacuum-Ultraviolet Light Absorption," *Journal of Chemical Physics*, Vol. 47, No. 9, 1967, pp. 3231–3240.

[7] Johannesen, N. H., Zienkiewicz, H. K., Blythe, P. A., and Gerrard, J. W., "Experimental and Theoretical Analysis of Vibrational Relaxation Regions in Carbon Dioxide," *Journal of Fluid Mechanics*, Vol. 13, Pt. 2, 1962, pp. 213–225.

[8] Simpson, C. J. S. M., Bridgman, K. B., and Chandler, T. R. D., "Shock-Tube Study of Vibrational Relaxation in Carbon Dioxide," *Journal of Chemical Physics*, Vol. 49, No. 2, 1968, pp. 513–522.

[9] Baganoff, D., "Experiments on the Wall-Pressure History in Shock-Reflection Processes," *Journal of Fluid Mechanics*, Vol. 23, Pt. 2, 1965, pp. 209–228.

[10] Baganoff, D., "Pressure Gauge with One-Tenth Microsecond Risetime for Shock Reflection Studies," *Review of Scientific Instruments*, Vol. 35, No. 3, 1964, pp. 288–295.

[11] Johannesen, N. H., Bird, G. A., and Zienkiewicz, H. K., "Theoretical and Experimental Investigations of the Reflexion of Normal Shock Waves with Vibrational Relaxation," *Journal of Fluid Mechanics*, Vol. 30, Pt. 1, 1967, pp. 51–64.

[12] Presley, L. L. and Hanson, R. K., "Numerical Solutions of Reflected Shock Wave Flowfields with Nonequilibrium Chemical Reactions," *AIAA Journal*, Vol. 7, No. 12, Dec. 1969, pp. 2267–2273.

[13] Hanson, R. K., "An Experimental and Analytical Investigation of Shock-Wave Reflection in a Chemically Relaxing Gas," SUDAAR 345, May 1968, Stanford Univ., Dept. of Aeronautics and Astronautics, Stanford, Calif., pp. 178–180, 254–261.

[14] Hanson, R. K., "Shock-Wave Reflection in a Relaxing Gas," *Journal of Fluid Mechanics*, Vol. 45, Pt. 4, 1971, pp. 721–746.
[15] Vincenti, W. G. and Kruger, C. H., Jr., *Introduction to Physical Gas Dynamics*, Wiley, New York, 1965.
[16] Hanson, R. K. and Baganoff, D., "Improved Fast-Response Pressure Gauge for Shock-Reflection Studies in Ionized Gases," to be published.
[17] Hanson, R. K. and Baganoff, D., "Shock-Tube Study of Vibrational Relaxation in Nitrogen Using Pressure Measurements," *Journal of Chemical Physics*, Vol. 53, No. 11, 1970, pp. 4401–4403.

SEPTEMBER 1971 AIAA JOURNAL VOL. 9, NO. 9

Measurements in Ablating Air-Teflon Boundary Layers

JOHN H. CHANG* AND R. E. CENTER†
Avco Everett Research Laboratory, Everett, Mass.

Theoretical descriptions of the detailed structure of an ablating air-Teflon laminar boundary layer predict CF_2 to be a major constituent in the boundary layer. This species has not been observed experimentally. This paper presents spectrally and spatially resolved uv thermal radiation measurements that demonstrate the presence of CF_2 in the stagnation point boundary layer of ablating Teflon cylinder. The experiments were performed in an arc facility which provided subsonic air or nitrogen jets at 2500–4500°K and $\frac{1}{40}$ atmospheric pressure. The state of the freestream was measured by the electron beam fluorescence technique.

I. Introduction

THE detailed structure of laminar ablating air-Teflon boundary layers has been the subject of many investigations.[1–4] Most of the experimental data has been reviewed in Ref. 3, which includes an analysis developed to describe the structure of the boundary layer. The analysis uses a partial equilibrium model for the air-Teflon chemistry which does not permit the formation of CF_3 and CF_4 within the boundary layer. The validity of the model was based on the excellent agreement between the measured and the theoretically predicted peak intensity of CO_2 radiation, its position in the boundary layer and the integrated intensity across the boundary layer. This theory further predicts the presence of COF_2 as a major radiator in air-Teflon boundary layers. Measurements of absolute intensities by Young, et al.,[4] were in good agreement with theoretical predictions. The analysis also predicts that CF_2 would be a major species in the boundary layer. This species has not been experimentally observed.

The work presented here was undertaken to demonstrate the existence of CF_2 in the air-Teflon boundary layers by spectrally resolved uv thermal radiation measurements in the stagnation point boundary layer of ablating Teflon cylinders. After demonstrating its presence, the spatial distribution of the CF_2 emission in the boundary layer was measured in order to provide additional information on the chemical processes in the boundary layer. A low-density d.c. arcjet facility was used to provide subsonic air or nitrogen jets at 2500–4500°K and $\frac{1}{40}$ atmospheric pressure. The state of the freestream gas was measured by use of an electron beam probe. The boundary-layer measurements were made at the stagnation point of a 1 cm diam by 1-cm long Teflon cylinder. By measuring on the axis of the jet, the problems of interference by the jet's mixing boundaries, the cold nozzle wall boundary layers and other jet nonuniformities were eliminated. In addition, the stagnation point provided both a laminar boundary layer and sufficient heat transfer for steady-state ablation to be rapidly reached over a wide range of arc operating conditions.

Received January 4, 1971; revision received May 13, 1971. This research was supported by the Advanced Research Projects Agency of the Department of Defense and Space and Missile Systems Organization, Air Force Systems Command, and was monitored by Space and Missile Systems Organization, Air Force Systems Command under Contract F04701-69-C-0122. The authors enjoyed many stimulating discussions with M. Camac. The identification of the CF_2 spectra was carried out by L. Young. The authors are also grateful to R. Rennie for his assistance in the operation of the arc facility.

* Formerly Senior Research Scientist, AVCO Everett Research Laboratory; presently Section Head, Fluid Mechanics Laboratory, TRW Systems Group, One Space Park, Redondo Beach, Calif.
† Principal Research Scientist.

II. Experimental Apparatus

A. Arcjet

The AERL low-density arcjet is a d.c.-battery-powered facility which produces a subsonic air jet at temperatures from 2500–4500°K and at a pressure of $\frac{1}{40}$ atmosphere. The input power is variable over the range of 30–80 kw. The air mass flow was approximately 1.5 g/sec and the flow velocity was 10^5 cm/sec. A schematic diagram of the arc is presented in Fig. 1. Nitrogen is introduced around the circumference of the 2% thoriated tungsten cathode. It flows around the cathode and into the anode section. This swirling flow stabilizes the arc by constricting the arc to the anode centerline. Oxygen is introduced downstream of the anode by means of twelve radial holes circumferentially placed at the entrance to the plenum chamber. The gases mix within the plenum chamber and the hot air exits through the 1.9-cm-diam nozzle. All internal components are water-cooled and, with the exception of the cathode, are constructed of copper. The arc is enclosed in the low pressure chamber, which is evacuated by a 500-cfm pumping system using a Stokes mechanical pump.

The gas power was determined by substracting the wall losses from the arc input power. These losses were obtained by measuring the temperature rise ΔT and the flow rate of the coolant water, $\dot{m}_{H_2O}$, through the arc. The enthalpy per unit mass of gas H was then given by

$$H = (VI - S\dot{m}_{H_2O}\Delta T)/\dot{m}_{air} \quad (1)$$

where V and I are the arc operating voltage and current,